A Low-Cost and Fast Vehicle Detection Algorithm With a Monocular Camera for Adaptive Driving Beam Systems

SHANGHONG LI AND **LINHUI ZHAO**

Department of Control Science and Engineering, Harbin Institute of Technology, Harbin 150001, China

Corresponding author: Linhui Zhao (zhaolinhui@hit.edu.cn)

ABSTRACT The adaptive driving beam headlamp system is helpful to solve the traffic safety problems caused by the abuse of high beams at night. The fundamental problem for the adaptive driving beam system is to detect and track the vehicles at specific night environment for light shape control. This paper proposes a new and efficient algorithm for detecting and tracking based on video collected by a low-cost camera. The related automobile regulations are analyzed for classifying the application scenarios of the adaptive driving beam system and summarizing the performance requirements of the algorithm. A standard CMOS camera mounted behind windshield captures the test video from different scenarios. Some preprocessing approaches are designed to optimize the captured video so that the algorithm can work independently on specific camera. The color and morphological characteristics of the rear lights are utilized to extract the rear lamps of the vehicle. The symmetry of rear lights is checked by a correlation coefficient method to pair the rear lamps and determine the vehicle ahead preliminary. Then, the Hungarian algorithm and Kalman filter are performed to track the multiple occurrences in two consecutive frames and correct the detection results. Finally, an estimation method is given for calculating the vehicle position in real world. The experiments are designed according to referred regulations and the test video is obtained from a low-cost camera mounted on test vehicles driving in specific scenarios. The experimental results demonstrate that the algorithm can get high detection rates and adaptability to the working condition of adaptive driving beam system. Moreover, the proposed algorithm has low time cost and can be applied in embedded devices of the vehicle.

INDEX TERMS Adaptive driving beam, image processing, rear lights recognition, video processing, system testing.

I. INTRODUCTION

Vehicle driving-beam headlamps are important for traffic safety since most driving environments are not illuminated at night. On the one hand, drivers need their driving beam to be brighter enough for visibility of the road ahead. On the other hand, the over-bright driving beam may cause dazzle of other road users. These two aspects are contradictory in nature. To solve this contradiction, the drivers need to manually switch the headlamps between the passing beam and the driving beam. However, manual operation is inconvenient and the passing beam cannot illuminate the road sufficiently under some conditions. Only the automatic driving beam with adjustable intensity and lighting-range can be the final solution. Adaptive Driving Beam (ADB) system is a realization of above functions. It goes beyond some auto-headlamp systems that switch between driving and passing beam automatically. Its principle is detecting the specific areas where overcoming or preceding vehicles appearing, reducing the light intensity in these areas or adjusting the pattern of driving beam. So that the other road users will not feel dizzy or uncomfortable, while drivers can get illumination of the road as much as possible. Some analyses in [1] estimated that such systems might reduce traffic crashes at night by 6% to 7% than switching driving beam manually.

To adapt the shape of driving beam dynamically, the ADB system needs sensors and corresponding algorithms to obtain the positions of vehicles in the front view as the input

The associate editor coordinating the review of this manuscript and approving it for publication was Shenghong Li.

signal for controller. Therefore, the performance of ADB system depends upon the capability of sensors and detecting algorithms directly. However, the increase of hardware performance is often accompanied by higher costs. Since the monocular camera has been the standard configuration in smart cars currently, developing faster algorithm on the existing camera is a lower cost method that can improve the software performance. In this paper, vehicle detecting and tracking algorithms are promoted for the specific needs of ADB system in scene of following vehicle ahead. The algorithm is developed on video captured by the monocular camera, which guaranteed the stability and compatibility of running on the vehicle platform. At the same time, it has a fast detection speed and a high success rate and then can provide effective input for the ADB system.

The rest of this paper is organized as follows: In *Section II*, the previous related work is briefly reviewed. *Section III* introduces the detecting algorithm of vehicle ahead based on image. *Section IV* introduces the vehicle tracking algorithm and the method of position estimation. *Section V* shows the testing results. And the conclusions are given in *Section VI*.

II. STATE OF THE ART

The current researches on ADB system primarily focus on the relevant laws and regulations, the driving modules and control strategies of vehicular headlamps. In [2], a vehicular headlamp that uses an LED matrix was stated to realize adaptive light shape adjustment. Its input of control modules defaults to the position of vehicles ahead, while the method of obtaining the position is not clearly indicated.

Although detecting algorithm of proceeding vehicle in nighttime is very important to the performance of ADB system, there is a lack of specialized research on it. Current researches on detecting algorithms were mostly conducted on Advanced Driving Assistance Systems (ADAS), such as collision warning. The requirements of ADAS for detection algorithms are different from the ADB system. The distance requirement of detection in ADAS is not far, and the accuracy requirement is higher compared with the ADB system.

The proposed detecting algorithms in existing researches for ADAS also have several limitations. Some of the algorithms were designed based on active sensors such as millimeter wave radar and LIDAR. A near infrared camera was utilized to implement detection in [3], and sonar sensors were employed in [4]. Such sensors are not normal configurations of mass-production vehicles that causes higher cost. Additionally, the detection distance of the low-cost sensors, such as ultrasonic radar or infrared sensor, is closer than the need of ADB system. Besides, some studies used cameras calibrated or modified in advance that have specific parameters to get better performance, like [5] and [6]. In [5], a standard camera with color filters and CMOS sensors was used to obtain front images. A method based on a perspective blob filter to detect vehicles during nighttime was proposed in [6]. However, these methods are difficult to use on different vehicle platforms. Therefore, getting rid of the dependence on hardware

and developing an image processing algorithm working on ordinary cameras are beneficial for considerable application range, low price and easy installation.

With a normal monocular camera, several detection methods for preceding vehicles at night were developed for ADAS in [7]–[12]. In [7], an algorithm was proposed for brake-light detection based on nakagami imaging method. The results indicate that the proposed algorithm can get good detection rate for brake lights. But its detecting speed cannot meet the real-time requirements. In [8] and [9], light source characteristics were used to segment the ambient light and object lights for traffic surveillance. Also, the algorithms in [7]–[9] were all developed on single pictures. In [10] and [11], videos were used for further analysis. The excellent performance of Kalman filter in vehicle tracking task was illustrated in [10]. In [11], a method to detect the suspected vehicle in each frame and a cross-frame algorithm were used to achieve vehicle tracking. Although their application scenarios are quite different from the ADB system, the ideas were instructive. In [12], vehicle detecting algorithms were summarized as two steps: the light screening step and the light pairing step. In the first step, the candidate rear lamps are separated from the background by color or brightness segmentation. In the second step, the extracted candidate rear lamps are paired and classified to obtain the position of the potential vehicles. This paper further expands on the basis of the two steps and propose a novel method that is aiming for the requirements of the ADB system.

Recently, machine learning have attracted extensive interest because of its great performance in target detection. However, due to low exposure conditions in ADB work scenes, features of vehicles ahead are not obvious and often confused with ambient lights. This may result in false detection [13]. In [14], a vehicle classifier based on tensor decomposition and support vector machine (SVM) was proposed for anti-collision detection during night driving. The method presented in [15] recommended that the images should be preprocessed before training and detecting. Therefore, using explicit rules and threshold-based methods also play a significant role in machine learning. Unlike the other powerful computing platforms, the computing and data transmission capacity of vehicle controllers are limited by the cost of such implementations. These limitations also need to be considered in the designed algorithm in this article.

Based on the above-mentioned researches, an embedded vehicle detection algorithm is designed based on an on-board camera in this paper. A low-cost color camera without special configuration is used as the sensor. The algorithm provides the control input of the ADB system. It uses the color, shape, symmetry and position features of the vehicle rear lamps from the night images to realize the detection. Then, using the Kalman filter and Hungarian algorithm to correct the detection result to realize the tracking of the vehicle ahead. Compared with the existing methods, this paper faces the needs of the ADB system, provides a low-cost and fast algorithm to solve the following problems: 1) Optimize night
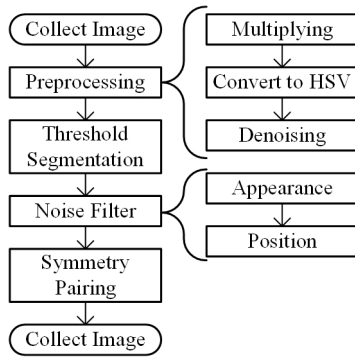
FIGURE 1. Structure of the detection algorithm.

image, filter ambient light, and extract vehicle rear lamps;
2) Realize multi-vehicle detection in complex night scenes;
3) Use video continuity to track and predict the vehicle ahead;
4) Estimate the position of the vehicle ahead.

III. REAR LAMPS DETECTION

This section analyzes regulations and utilizes the characteristics of the vehicle lighting systems, such as color threshold, shape, and symmetry, to establish a detection algorithm that extracts tail lights from background. The structure of the proposed detection algorithm is described as in Fig.1, which includes image preprocessing, threshold segmentation, noise filter and symmetry pairing.

A. SCENARIOS AND REQUIREMENTS

Due to the particularity of vehicle systems, the corresponding automobile regulations must be checked first. It helps summarizing the characteristics and specifies the testing method for the ADB system. After studying standards of China, the European Union and the United States, the relevant content is found basically the same. Since the EU Automobile Regulations describes more accurately, this article will mainly refer EU standards. The two most relevant regulations are "Uniform Provisions on the Certification of Motor Vehicles for the Installation of Light Signal Devices" (referred as E.C.E Reg.48) and "Uniform Provisions on Approving the Installation of Automotive Adaptive Front Lighting Systems" (referred as E.C.E Reg.123). The different application scenarios and the performance requirements stated in the two regulations will be considered in this article.

For the ADB system, when the ambient light brightness is lower than a certain value (E.C.E Reg.48 recommends 7000 lx), the headlamps will be turned on and the system will control the light shape according to the results of vehicle detection in the front. Therefore, the vehicle detection algorithm needs to adapt to all environments of night driving. However, the characteristics of different roads displayed on the images are not exactly the same. Finding the characteristics of all these scenes is not an easy task. Therefore, the above-mentioned regulations are studied to classify and analyze the complex scenarios. The regulation E.C.E Reg.48 specifies that the adaptive high beam system

needs to be tested on certain road types, including urban areas, multi-lane road, and country road.The main difference between these scenarios is the exposure conditions and traffic densities. At the same time, the tested length and the corresponding speed of different road type are given. According to these test conditions, field driving at night on these three road types are conducted to build a test library. The RGB color images of vehicle ahead are captured by a CMOS camera mounted on the windshield of a test car.

After collection of the images of vehicle ahead, five scenarios can be summarized as follows:

(1) The overall image contrast is high, and the center area of the front vehicle light appears white due to overexposure.

(2) There is a large-scale halo in the rear lamps area of the same direction vehicle with the edge beyond the car body. The halo near the center shows a more uniform red, and the edge shows rose red or orange.

(3) The shape of the rear lamps is regular, basically showing complete left-right symmetry.

(4) Vehicle rear lamps on some curved road sections appear distorted or blocked.

(5) The area of the rear lamps of the vehicle and the center coordinate spacing of the left and right rear lamps are related to the position and distance of the vehicle in the image.

These different scenarios have the same problem of insufficient lighting. Without configuring the camera, images need to be preprocessed. For overexposure, scattering, and other issues, special consideration should be given. The vehicles ahead are primarily visible by their red-color rear lights especially for vehicles far away. All vehicles will differ in appearance with different designs of rear lamps. Regulation E.C.E Reg.48 states that the rear lights should be installed in pairs. Therefore, the rear lamps must have symmetry to the center axis of the vehicle when viewed from the rear, which is a useful detection characteristic. To prevent the rear lamps from being confused with other lights, E.C.E Reg.48 limits the threshold range of red light emitted by the rear lamps in the CIE 1931 colorimetric space. The red boundary is defined by the following inequality (1) as:

$$y \leqslant 0.335$$
$$y \geqslant 0.980 - x \qquad (1)$$

where x, y are coordinates in CIE color space. Unlike the previous detection methods manually define rear lights color based on experience, this article gives a clearer red threshold in conjunction with regulations.

Regulation E.C.E Reg.48 sets out the requirements for sensors of ADB system, including the target and the detectable distance. The vehicle detection algorithm and a CMOS camera act as a sensor providing input information for the ADB system. Therefore, the sensor requirements in the regulations are suitable to this algorithm. The regulation states that the sensor should be able to detect the red rear lights signal at the rear of the vehicle in the same direction at least 100 m.

TABLE 1. Test requirements for light intensity and vehicle distance of ADB system.

Test Point	Maximum light intensity (cd)
Oncoming vehicles at 50 m	625
Oncoming vehicles at 100 m	1750
Oncoming vehicles at 200 m	5450
The vehicle ahead in the same direction is at 50 m	1850
The vehicle ahead in the same direction is at 100 m	5300
The vehicle ahead in the same direction is at 200 m	16000

Regulation E.C.E Reg.123 claims the relationship between the maximum light intensity of the high beam and the distance between the vehicle ahead in test of the ADB system. As shown in Table 1, the test points are set at 50 m, 100 m, and 200 m in the same direction. Therefore, the vehicle detection algorithm should have the ability to detect vehicles 200 m ahead and be able to distinguish vehicles within 0-50 m, 50 m-100 m, and above 100 m.

These application scenarios and performance requirements provides guidelines for the design of the vehicle detection algorithm in the following.

B. SUSPECTED REAR LAMPS EXTRACTION

The first problem stated in section III is the high image contrast and overexposure. The central area of rear lamps produces bright white, and red halo exists beyond range of rear lamps. Therefore, it is necessary to balance the color gradation of the image, darken the overexposed part, and filter out the halo beyond the range of the rear light. This article chooses the multiplying algorithm to optimize the image. Multiplying is a commonly used image blending mode. The effect is similar to overlapping original image with a covering image, like two transparent slides, observing them with illuminating by a light source. Due to the content on the covering image, the resulting of multiplying is generally darker than original images. Since choosing pure color pictures results in the loss of original information, the original image is chosen as the covering image. The transformation formula is as follows:

$$s = \frac{s_0^2}{255} \quad (2)$$

where s_0 is the pixel value in the original image, and s represents the corrected pixel value. Compared with color filter, linear deepening and other processing methods, multiplying is more suitable for processing night images with lights. It can compress the pixel range of the dark part and retain the color information of the original image without distortion. At the same time, this algorithm has stronger versatility and is simple, fast, and suitable for implementation in embedded devices. After preprocessed, the white areas caused by overexposure in the center of rear lamps are reduced. As can be seen from the comparison in Fig.2, the red halo which beyond the body part gets darker, the brighter parts in rear lights range

(a) The original image (b) After multiplying

FIGURE 2. Comparison before and after multiplying.

are kept. And the interference of the dim red light source in the environment is filtered.

Section II introduced some previous rear lamps detection systems. Most of them only use experimental data to determine the rear light threshold. This way often makes the threshold range larger or having deviation. In this article, the red boundary of the rear lamps will be studied according to the regulation E.C.E Reg.48. The limits from CIE 1931 colorimetric space are used as a benchmark. Then certain adjustments based on experimental data are operated to eliminate the color cast. Due to the boundaries given in the regulation E.C.E Reg.48 cannot be used directly in calculation, the limits need to be converted to the color space expected to perform threshold segmentation. In this article, Hue-Saturation-Value (HSV) color space is chosen for further processing. In which, H represents hue or tint as the angle (0-360), S represents saturation or shade as radius (0-1), and V represents value or tune as perpendicular height (0-1). Compared with other color spaces, HSV color space has the following advantages:

(1) It describes each pixel by separating hue and saturation. Compared with color spaces with three primary colors, such as RGB, this description is closer to the perceivable colors by human eyes. Therefore, it is easier to adjust threshold parameters in HSV while conducting experiments.

(2) It is a commonly used digital image model. Some color spaces establishing for human eyes, such as Lab and LXYZ, describe colors more detailed. However, they are not convenient to use in computers.

(3) HSV uses a conical space model, which makes it easier to observe the color distribution. Compared with other color spaces that separate color by hue and saturation, such as HSI, it is more intuitive.

Using RGB space as an intermediary, the coordinates xyz in CIE space can be converted to values in HSV space by the following formulas [16]:

$$X = \frac{Y}{y}x$$
$$Z = \frac{Y}{y}(1 - x - y)$$
$$\begin{bmatrix} R \\ G \\ B \end{bmatrix} = \begin{bmatrix} 0.4185 & -0.1587 & 0.0828 \\ -0.0912 & 0.2524 & 0.0157 \\ 0.0009 & -0.0025 & 0.1786 \end{bmatrix} \begin{bmatrix} X \\ Y \\ Z \end{bmatrix} \quad (3)$$

where x, y are coordinates in CIE color space and X, Y, Z are intermediate variables in Calculating. R, G, B are values of RGB color space after gamma correction with $\gamma = 2.2$

TABLE 2. Rear light thresholds in HSV.

	Minimum	Maximum
Hue	342°	9°
Saturation	0.4645	0.2
Value	0.2	1.0

TABLE 3. The average error threshold range of the rear lights of the sample picture.

|	Minimum	Min in 8bit	Maximum	Max in 8bit
Hue	340°	171-181	10°	0-5
Saturation	0.4645	118	0.98	250
Value	0.2	50	1.0	255

in linear texture. Then RGB color space is converted to HSV color space by following formulas (4):

$$\Delta = max(R, G, B) - min(R, G, B)$$
$$C = max(R, G, B)$$
$$H = \begin{cases} 0, & if\ \Delta = 0 \\ 60 \times (\dfrac{G-B}{\Delta}\ mod\ 6), & if\ C = R \\ 60 \times (\dfrac{B-R}{\Delta}\ mod\ 6 + 2), & if\ C = G \\ 60 \times (\dfrac{R-G}{\Delta}\ mod\ 6 + 4), & if\ C = B \end{cases}$$
$$S = \begin{cases} 0, & if\ C = 0 \\ \dfrac{\Delta}{C}, & if\ C \neq 0 \end{cases}$$
$$V = C \tag{4}$$

where H, S, V are the final values converted from the CIE color space to the HSV color space. Combined with equation (1), the red boundaries in the regulation E.C.E Reg.48 in HSV color space are shown in Table 2.

The above threshold also needs to be adjusted according to the experimental data of the collected samples. The rear lamps with typical characteristics in sample images are manually cropped. The pixel data of these areas is analyzed to obtain the average pixel value of the rear lamps in HSV color space. After the comparison, it can be seen that the threshold of most samples is within the range given by regulations. Due to the influence of ambient light in some urban road sections, the hue range deviates to the orange range. Therefore, the final hue range need to be expanded. After adjusting, the final rear light thresholds in HSV are shown in Table 3. Due to the HSV image is stored in the computer with 8bit depth, Table 3 also gives the threshold ranges used in the algorithm.

From the test results of the sample pictures, the threshold range obtained by this method is more accurate than just experimental studies. It can better eliminate the interference from other red lights and improve the detection success rate. Fig.3 shows the binary image after segmenting the red area. It can be seen that the rear lamps have been well separated from the original image. Most of the ambient light interference has been filtered. A pair of obvious rear lamps areas and some small areas of noise exist simultaneously. To further reduce the noise area, it is necessary to detect rear

(a) The original image (b) Red threshold extraction result
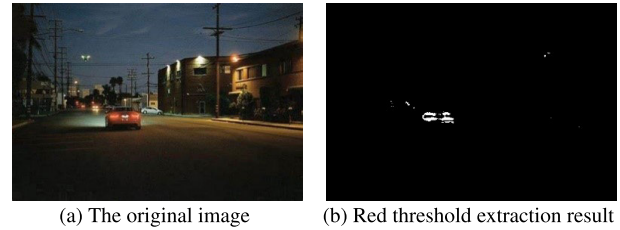
FIGURE 3. The binary image from the original image through red threshold extraction.

lamps according to other characteristics and match pairs to determine the vehicle position. The detecting and matching method will be discussed in the following subsection.

C. REAR LAMPS SCREENING AND MATCHING
In addition to color, area, shape and symmetry are also important features for detection. This subsection analyzes these features through connected component obtained from the above binary image. Connected component is a collection of adjacent pixels with the same pixel value in the binary image. The essence of connected component analysis is to combine similar individual pixels to find the properties of the entire set, including shape, boundary, area, etc. Commonly used methods to obtain connected component include seed-filling method and two-pass method. Through comparative tests, it is found that the computational speed of the two-pass method is about ten times faster than the seed-filling method. Therefore, the two-pass method is used in this study.

Since the camera is mounted in a fixed position on the vehicle body, the target vehicles usually do not appear in the upper left and right corners of the image. First, the connected components appearing in these areas are deleted according to this position nature. The specific boundary is based on experiments of sample images. The next step is to remove noise based on area of connected component. The area of the noise caused by ambient light interference or color cast is generally small, which among tens pixels in 480p videos. However, the rear lamps of some distant vehicles are also within this range. Selecting a fixed absolute area critical value to filter connected components may cause some rear lights to be deleted. Therefore, in this paper, one-eighth of the largest connected component in area will be used as the critical value. Such a relative value can have a better filtering effect regardless of whether the vehicle ahead is far or near. Finally, the connected components are filtered according to the shape information of the rear lights. Although there is no regulation restricting the shape and the design styles of rear lamps, the aspect ratio of most rear lamps bounding box is regular. In order to filter interference in strip shape caused by scattering or reflection, the ratio of the horizontal length to the vertical width of the connected component is required to be between 0.4 and 5. Due to existence of some vertical design rear lamps such as Volvo, the lower bound of the ratio is set to a smaller value of 0.4. After the above operations, the results of the example in Fig.3 are shown in Fig.4. It can be seen that the environmental noise has been well filtered. The
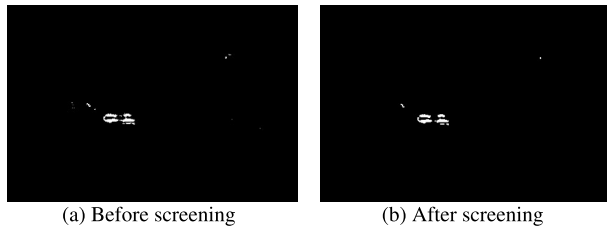
| (a) Before screening | (b) After screening |

FIGURE 4. Comparison of binary graph before and after screening.

| (a) Result of sample image | (b) Vehicle in long distance |

FIGURE 5. Detection results.

interference from the vehicle body and the ground reflection has been deleted. And the bright block outlines of the rear lamps in the image are clearer.

In addition to the above-mentioned features, the rear lamps have another important feature, which is the symmetry to the center axis of the vehicle. Due to the requirements in regulation, the rear lamps must be installed strictly in pairs. According to this character, some interference that in similar size and shape but exist alone can be filtered. It is worth noting that some vehicles install a high-position brake light at the top center of the rear window. It emits exactly the same red as the rear light. Since this brake lamp does not light up during normal driving, most algorithms based on the rear lamps do not consider its impact. However, it causes deviations in position judgment in our experiments while the vehicle detected braking. Generally, the high-position brake lamps install on the different horizontal line and no other red light is symmetrical to it. Therefore, using symmetry judgment can effectively avoid this deviation. Checking all connected components appearing in the image, two of them that meet the following conditions are extracted for symmetry detection:

(1) The coordinates of center points are close to the same horizontal line;

(2) The area difference is less than one-eighth of the larger connected component;

(3) The distance between center points of the two connected components does not exceed 7 times the horizontal width of the larger connected component;

Considering the balance of calculation accuracy and complexity, symmetry detection is performed in gray scale of the original image. For connected components that meet the above conditions, their corresponding regions in the gray scale image will be clipped. These two regions are essentially two digital matrices. Therefore, the Pearson correlation coefficient method, which is commonly used to measure matrices correlation, is selected here for symmetry detection. After horizontally mirroring one region, two regions are expanded to the same size, and denoted as matrix A and B respectively. Then, the Pearson correlation coefficient ρ between them can be calculated as follows [17]:

$$\rho(A, B) = \sum_{x,y} \frac{(A_{x,y} - \bar{A})(B_{x,y} - \bar{B})}{\sigma_A \sigma_B} \qquad (5)$$

where $A_{x,y}$ and $B_{x,y}$ represent the gray value of x row and y column in matrix A and B respectively. $\bar{A}$ and $\bar{B}$ represent
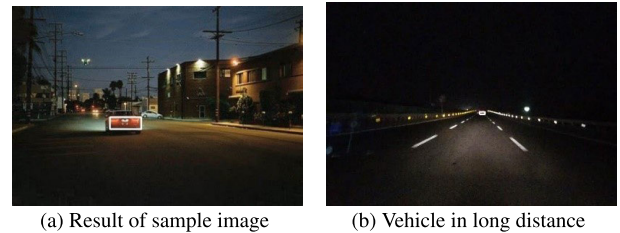
mean values of all elements in matrix A and B respectively. σ_A and σ_B are the standard deviations of matrix A and B respectively.

The absolute value of ρ is between 0 and 1. When it is closer to 1, the matrix cross-correlation is stronger. Generally, two matrices, whose ρ value is greater than 0.8, are cross-correlated extremely strong. And a ρ value between 0.6 and 0.8 indicates the cross-correlation are strong. Derived the value from the Pearson correlation coefficient for valid vehicle rear lamps in sample images, the result in symmetry detection threshold is $\rho_{min} = 0.75$. Two connected components with a correlation coefficient greater than 0.75 will be regarded as two rear lamps of the same car and will be marked. The algorithm continues checking the remaining connected components that meet the conditions. The marked one will be skipped to prevent repeated detection. Fig.5 shows the results of the sample images in Fig.2 and a situation in long distances.

As can be seen from Fig.5, the algorithm performs well in different distances and road types. Compared with other rear lamps detection systems, the proposed method in this study utilizes color and shape information, which is sensitive to threshold segmentation, and also symmetry information, which is independent of threshold segmentation. These are useful for the accuracy and stability of detection. The algorithm can also detect the situation of multiple vehicles ahead, which is not achieved in many previous studies.

IV. TRACKING AND POSITION ESTIMATION

The algorithm described in Section III works on the single image, which detects vehicles ahead at night in high successful rate. However, it was observed from preliminary testing that some failures happened during high speed driving, which is mainly because of images distortion and rear lamps obscured caused by shaking camera. To better smooth these interference, the association between video frames are explored to correct the result from Section III. The method in this section performs tracking through the Kalman filter to improve the robustness of the system. Also, the Hungarian algorithm is applied to matching detection results cross-frame especially in multi-vehicle situation. Following the correction for the previous results, a position estimation method is proposed to provide distance output for the ADB system.

A. TRACKING

Prior to designing tracking process, some basic assumptions are made for the vehicle motion to satisfy the requirements

of the Kalman filter. The bounding box of the vehicle in uniform linear motion remains unchanged. The speed and acceleration of the target vehicle moving in the image are smoothly changing. The noise of the detection result and the change process of the vehicle state conform to the zero mean noise distribution. Once the positions of vehicles ahead in the first frame had been decided upon, the bounding box of each vehicle (u, v, w, h) was stored in memory. u and y represent coordinate of the center point. w and h represent width and height of the bounding box. These are arranged into a column to form the first state vector $\vec{X}_k$ for the Kalman filter. First, the prediction process of the Kalman filter is carried out, including prior estimation $\vec{X}_{k+1}^k$ based on state transition relationship and prediction of the new state error covariance matrix P_{k+1}^k [18]:

$$
\begin{aligned}
\vec{X}_{k+1}^k &= F\vec{X}_k \\
P_{k+1}^k &= FP_kF^T + Q
\end{aligned}
\tag{6}
$$

where k is the discrete moment corresponding to the current frame, and F is the state transition matrix. According to the assumption, F is chosen as an identity matrix. Q is the process noise covariance matrix, generally a diagonal matrix, represents the reliability of the system.

When the detection of the following frame completed, the measured result $bbox_m$ is matched with the predicted result $bbox_s$ through the Hungarian algorithm [19]. Define IoU as:

$$
IoU = \frac{bbox_m \cap bbox_s}{bbox_m \cup bbox_s}
\tag{7}
$$

which means intersection over union, represents the difference between two bounding boxes. It fused the similarities of the location and the size at the same time. The predicted result and the measured result are regarded as the same vehicle from different frames if IoU is greater than a threshold IoU_{min} while performing the Hungarian algorithm. When the value of IoU is 1, the measured bounding box and prediction bounding box overlap perfectly. The matching result is recognized as acceptable if IoU value is greater than 0.5. Combined with the performance in the elementary tests, the threshold value is set as $IoU_{min} \geq 0.6$ to obtain a more rigorous matching result. Once the Hungarian algorithm was completed, each measured bounding box in current frame is regarded as the measurement state $\vec{z}_{k+1}$ in the Kalman filter. The Kalman gain of current moment K_{k+1}, the ratio of estimator variance to measurement variance, is calculated by:

$$
K_{k+1} = P_{k+1}^k H^T (HP_kH^T + R)^{-1}
\tag{8}
$$

where H is the system measurement matrix, R is the measurement noise covariance matrix. Since the measured value is the same form as state vector, H is an identity matrix. R and Q are diagonal matrices. Their diagonal values determine the weighing of the predicted value and the measured value. Generally, the larger value of Q represents the higher weighing of the measured value in the update process. Larger

value of R means less weighing on measured value. These two values need to be adjusted in the experiments to get better tracking results. The tuning method in this paper is provided as follows: First a smaller value 0.001 is selected as the value on the diagonal of Q for rapid convergence. The value of R is then adjusted. The final value of $R = 0.12$ is suitable for tracking responsive and remaining stable. Finally, the Kalman filter update process is performed to correct the predicted value and error covariance:

$$
\begin{aligned}
\vec{X}_{k+1} &= \vec{X}_{k+1}^k + K_{k+1}(\vec{z}_{k+1} - H\vec{X}_{k+1}^k) \\
P_{k+1} &= P_{k+1}^k - K_{k+1}HP_{k+1}^k
\end{aligned}
\tag{9}
$$

where $\vec{X}_{k+1}$ is the state vector in current frame, represents the final correction result combining the predicted vector $\vec{X}_{k+1}^k$ from previous frames and the measured value $\vec{z}_{k+1}$ from detection algorithm. Next, $\vec{X}_{k+1}$ and P_{k+1} are used to repeat the prediction process of the Kalman filter for the predicted vector $\vec{X}_{k+2}^{k+1}$ in the next frame. With the iteration of the Kalman filter, the tracker remains stable during interference.

B. POSITION ESTIMATION

The algorithm presented above determines the bounding boxes of vehicles ahead in the image represented by (u, v, w, h). This subsection estimates the real-world coordinates of the target vehicle through assumptions and calibration experiments. The world coordinate system is established with the projection of the front bumper on the ground as the origin O_W. The Z-axis is forward along the driving direction of vehicle, the X-axis is toward left perpendicular to the driving direction, and the Y-axis is vertically upward. The light emitted by the vehicle passes through the camera aperture, forms its inverted real image on the internal CMOS sensor. Therefore, in the world coordinate system, the coordinates of the target vehicle represented by (X_W, Y_W, Z_W), the coordinates of the camera aperture represented by (X_{Wc}, Y_{Wc}, Z_{Wc}), and the coordinates of the vehicle image on the CMOS sensor represented by (x, y, Z_f), should be on the same straight line. The line equation is as follows:

$$
\frac{X_W - X_{Wc}}{X_W - x} = \frac{Y_W - Y_{Wc}}{Y_W - y} = \frac{Z_W - Z_{Wc}}{Z_W - Z_f}
\tag{10}
$$

where $Z_f = Z_{Wc} - f$, and f represents the focal length of the camera. The real image on CMOS sensor is discretized to digital pixel image. The point (x, y, Z_f) in the real image in world coordinate system corresponds to the pixel (u, v) in the digital image as follows:

$$
\begin{aligned}
x - X_{Wc} &= (u - u_0)d_x \\
y - Y_{Wc} &= (v - v_0)d_y
\end{aligned}
\tag{11}
$$

where (u_0, v_0) is the center point of the image, d_x and d_y represent the real size of one pixel on the CMOS sensor. d_x, d_y and the aforementioned focal length f are the internal parameters of the camera, which can be obtained through calibration experiments [20]. The above equations are not enough to realize the transformation from (u, v) to (X_W, Y_W, Z_W). Since

this is essentially an inverse projection, which cannot achieve without another dimension. Hence, this article sets some assumptions based on the characteristics of the rear lamps. The mounted height of rear lamps has limitations, not less than 350 mm nor more than 1, 500 mm above the ground [17]. Considering the conservative of detection, the rear lamps are assumed locating on the plane defined by $Y_W = 400$ mm for passenger cars.

Combining the equations (10) and (11), the concerned vehicle position X_W and Z_W can be solved. The assumption may cause errors in some complicated road conditions. But the calculation cost is low and the algorithm is independent on the calibration experiments. Moreover, the estimated result can be corrected utilizing the following method.

Generally, the width of vehicle is 1800 mm and no more than 2000 mm for all passenger cars. On this basis, the distance between the center points of two rear lamps is set as $d = 2000$ mm considering the width and conservative. The following estimation is made by utilizing above assumption and similarity between the object and the real image:

$$Z_W = \frac{d \cdot f}{w \cdot d_x} \qquad (12)$$

where w is the width of bounding box. This method estimates the relative distance Z_W of the vehicle ahead. Due to the more stable assumption given above, it can be used as a correction estimation to assist the aforementioned algorithm.

V. EXPERIMENTAL RESULTS

Experimental videos were captured using a CMOS camera mounted on the windshield inside the test car. It can shoot video in 720 p and 30 Hz format. The screen pixel size is 1280*720. The videos with vehicles appearing totaled more than 3 hours in field tests. According to the requirements of testing road types in regulations, these videos were manually edited and categorized into three sets: 10% urban areas, 20% multi-lane road, and 70% country road. The speed of the test car ranged from 0 to 100 km/h. In most tests, the time cost of this algorithm in one frame is among 20 ms. Therefore, it can work frequently on the hardware equipment of existing vehicles.

To check the detection rate of the proposed algorithm, 1000 frames containing vehicles were intercepted from the test videos as samples. These frames were manually checked whether the algorithm correctly gives the bounding box of the vehicle. The number of frames with successfully detection to the total number of frames is counted as the detection rate. Table 4 presents the detection rate segmented according to the road type and distance range. In addition, 181 frames containing multiply vehicles is counted separately. The detection rate is 85.1%. It is noted that the overall detection rate is over 91%. The algorithm performs well in driving scenarios of country road and multi-lane road. At 50 meters to 100 meters, the distance where most dazzling occurs, the detection accuracy is better. In scenarios of urban road, the algorithm performs mediocre. This is because the lighting environment of
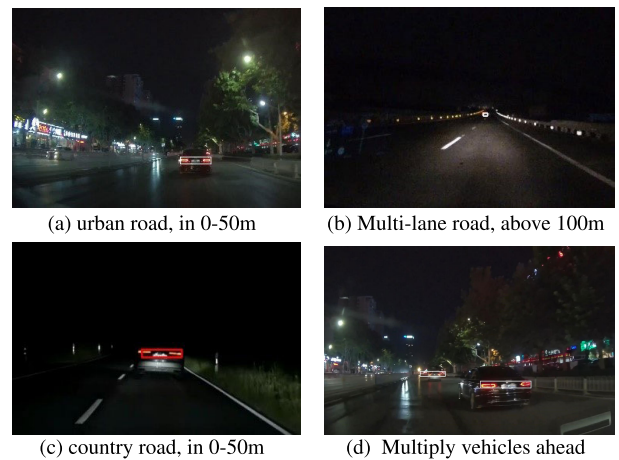

| (a) urban road, in 0-50m | (b) Multi-lane road, above 100m |
| (c) country road, in 0-50m | (d) Multiply vehicles ahead |

FIGURE 6. Result of test samples.

TABLE 4. The summary of experimental results by distance and road type.

Road type	Distance			
	0-50 m	50-100 m	Above 100 m	Total
Urban road	41/47	30/39	10/16	81/102
	87.2%	76.9%	62.5%	79.4%
Multi-lane road	76/83	105/115	58/62	239/260
	91.6%	91.3%	93.5%	91.9%
Country road	119/123	257/276	213/239	589/638
	96.7%	93.1%	89.1%	92.3%
Total	236/253	392/430	281/317	919/1000
	93.2%	91.2%	88.6%	91.9%

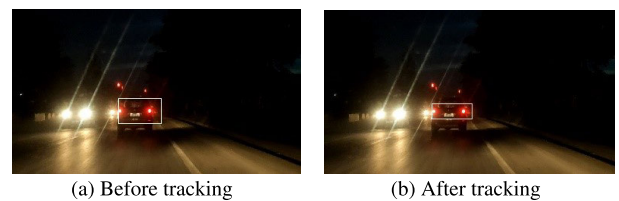| (a) Before tracking | (b) After tracking |

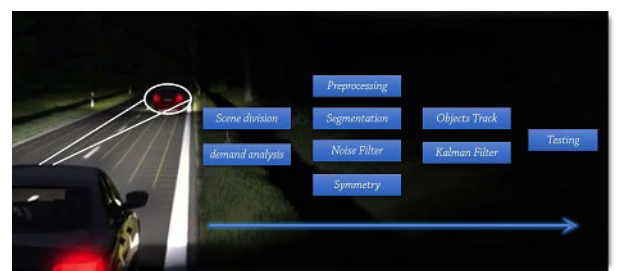**FIGURE 7.** Optimization effect of tracking algorithm.

FIGURE 8. Main work of this article.

the urban road is more complicated with various signs and signals emitted lights. This problem will be further solved in subsequent research. Some detection results of sample frames are shown in Fig.6.

To verify whether the tracking algorithm based on the Kalman filter is effective, the Kalman filter in the algorithm is shielded. Experimental videos were tested under the new algorithm. A sample frame is chosen to display the role of the Kalman filter. The comparison of whether applying the Kalman filter is as shown in Fig.7.

It can be seen intuitively that the Kalman filter corrected the bounding box of the vehicle. In Fig.7(a), the bounding box over the range of vehicle because of the ambient light interference. This situation did not happen in the frames before. Therefore, the Kalman filter corrected it according to the predicted data from previous frames. It can be concluded that the application of the Kalman filter on the basis of detection algorithm effectively improves the performance.

VI. CONCLUSION

In this paper, a detection algorithm for ADB system using videos captured by a CMOS camera was proposed. The main work of this article is shown in Fig.8. The frames of videos were preprocessed and performed segmentation in HSV color space. Red threshold was derived from E.C.E regulations and adjusted experimentally. The feature of rear lamps, such as position and shape, were utilized to filter the interference. The symmetry of rear lamps was checked through the Pearson correlation coefficient to identify the target vehicles. Based on the continuity of videos, a tracking algorithm was implemented by the Kalman filter and the Hungarian algorithm to improve the robustness and correct the detection result. Finally, the position of the vehicle ahead was estimated provided to the ADB system as a credible input signal. This paper also carried out the on-road field testing. The results indicated that the proposed algorithm can work well in different situation with high detection rate.

The main advantages of the algorithm are stability, high efficiency and no hardware dependency. The results of the test and the cost of running time have demonstrated that the algorithm has high robustness, high detection rate and outstanding detection speed. When applying this algorithm on different types of cameras, it only needs the parameters of the camera to initialize, and then can be accessed in. The algorithm can get satisfied inputs for the ADB system on common 720 p-resolution cameras. The detection distance and detection accuracy will improve with the increase of resolution. In future work, we will consider the interference from different weather condition and find a more accurate method of position estimation. Also, the control method of the high beam will be designed to realize the ADB system.

REFERENCES

[1] J. Bullough, "Adaptive high beam systems: Visual performance and safety effects," SAE Tech. Paper 2014-0431, vol. 2014, doi: 10.4271/2014-01-0431.

[2] Y. Qu, W. Shu, and J. S. Chang, "A monolithic I2 V2-controlled dual-phase LED matrix driver for automotive adaptive driving beam (ADB) headlighting," in *Proc. IEEE Custom Integr. Circuits Conf. (CICC)*, Austin, TX, USA, Apr. 2019, pp. 1–4, doi: 10.1109/CICC.2019.8780322.

[3] H. Kim, S. Kuk, M. Kim, and H. Jung, "An effective method of head lamp and tail lamp recognition for night time vehicle detection," *World Acad. Sci., Eng. Technol., Int. J. Elect., Comput., Energetic, Electron. Commun. Eng.*, vol. 4, no. 8, pp. 1255–1258, 2010.

[4] S. Kim, S.-Y. Oh, J. Kang, Y. Ryu, K. Kim, S.-C. Park, and K. Park, "Front and rear vehicle detection and tracking in the day and night times using vision and sonar sensor fusion," in *Proc. IEEE/RSJ Int. Conf. Intell. Robots Syst.*, Edmonton, Alta., Canada, 2005, pp. 2173–2178.

[5] R. O'Malley, E. Jones, and M. Glavin, "Rear-lamp vehicle detection and tracking in low-exposure color video for night conditions," *IEEE Trans. Intell. Transp. Syst.*, vol. 11, no. 2, pp. 453–462, Jun. 2010.

[6] T. Schamm, C. von Carlowitz, and J. M. Zöllner, "On-road vehicle detection during dusk and at night," in *Proc. IEEE Intell. Vehicles Symp.*, Jun. 2010, pp. 418–423.

[7] D.-Y. Chen, Y.-H. Lin, and Y.-J. Peng, "Nighttime brake-light detection by Nakagami imaging," *IEEE Trans. Intell. Transp. Syst.*, vol. 13, no. 4, pp. 1627–1637, Dec. 2012, doi: 10.1109/TITS.2012.2199983.

[8] W. Zhang, Q. M. J. Wu, G. Wang, and X. You, "Tracking and pairing vehicle headlight in night scenes," *IEEE Trans. Intell. Transp. Syst.*, vol. 13, no. 1, pp. 140–153, Mar. 2012, doi: 10.1109/TITS.2011.2165338.

[9] Y.-L. Chen, B.-F. Wu, H.-Y. Huang, and C.-J. Fan, "A real-time vision system for nighttime vehicle detection and traffic surveillance," *IEEE Trans. Ind. Electron.*, vol. 58, no. 5, pp. 2030–2044, May 2011.

[10] V. H. Pham and D. H. Le, "A two-stage detection approach for car counting in day and nighttime," in *Information Systems Design and Intelligent Applications*. Singapore: Springer, 2018, pp. 159–171.

[11] A. Almagambetov, S. Velipasalar, and M. Casares, "Robust and computationally lightweight autonomous tracking of vehicle taillights and signal detection by embedded smart cameras," *IEEE Trans. Ind. Electron.*, vol. 62, no. 6, pp. 3732–3741, Jun. 2015, doi: 10.1109/TIE.2015.2400420.

[12] A. Zaarane, I. Slimani, W. Al Okaishi, I. Atouf, and A. Hamdoun, "An automated night-time vehicle detection system for driving assistance based on cross-correlation," in *Proc. Int. Conf. Comput. Syst. Collaboration Big Data, Internet Things Secur. (SysCoBIoTS)*, Casablanca, Morocco, Dec. 2019, pp. 1–5, doi: 10.1109/SysCoBIoTS48768.2019.9028038.

[13] R. K. Satzoda and M. M. Trivedi, "Looking at vehicles in the night: Detection and dynamics of rear lights," *IEEE Trans. Intell. Transp. Syst.*, vol. 20, no. 12, pp. 4297–4307, Dec. 2019, doi: 10.1109/TITS.2016.2614545.

[14] H. Kuang, L. Chen, L. L. H. Chan, R. C. C. Cheung, and H. Yan, "Feature selection based on tensor decomposition and object proposal for night-time multiclass vehicle detection," *IEEE Trans. Syst., Man, Cybern. Syst.*, vol. 49, no. 1, pp. 71–80, Jan. 2019, doi: 10.1109/TSMC.2018.2872891.

[15] K. He, J. Sun, and X. Tang, "Single image haze removal using dark channel prior," *IEEE Trans. Pattern Anal. Mach. Intell.*, vol. 33, no. 12, pp. 2341–2353, Dec. 2011.

[16] E. Dubois, "The structure and properties of color spaces and the representation of color images," in *The Structure and Properties of Color Spaces and the Representation of Color Images*. San Rafael, CA, USA: Morgan & Claypool, 2009.

[17] J. Benesty, J. Chen, and Y. Huang, "On the importance of the pearson correlation coefficient in noise reduction," *IEEE Trans. Audio, Speech, Language Process.*, vol. 16, no. 4, pp. 757–765, May 2008, doi: 10.1109/TASL.2008.919072.

[18] W. Zhou and J. Hou, "A new adaptive robust unscented Kalman filter for improving the accuracy of target tracking," *IEEE Access*, vol. 7, pp. 77476–77489, 2019, doi: 10.1109/ACCESS.2019.2921794.

[19] H. Karunasekera, H. Wang, and H. Zhang, "Multiple object tracking with attention to appearance, structure, motion and size," *IEEE Access*, vol. 7, pp. 104423–104434, 2019, doi: 10.1109/ACCESS.2019.2932301.

[20] X. Gong, Y. Lv, X. Xu, Z. Jiang, and Z. Sun, "High-precision calibration of omnidirectional camera using an iterative method," *IEEE Access*, vol. 7, pp. 152179–152186, 2019, doi: 10.1109/ACCESS.2019.2945635.
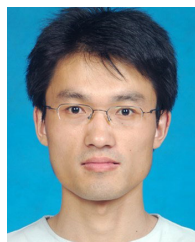
SHANGHONG LI was born in Lanzhou, China, in 1997. He received the B.S. degrees in automation from the Harbin Institute of Technology, Harbin, China, in 2020, where he is currently pursuing the M.S. degree in control science and engineering with the Department of Control Science and Engineering.

His research interests include vehicle dynamics and control, image processing, and self-adaptive control.

LINHUI ZHAO received the B.S. degree in automation from Harbin Engineering University, in 2003, and the M.S. and Ph.D. degrees in control science and engineering from the Harbin Institute of Technology, Harbin, China, in 2006 and 2009, respectively.

He is currently an Associate Professor with the Department of Control Science and Engineering, Harbin Institute of Technology. His research interests include vehicle dynamics and control, model predictive control, and nonlinear estimation.

• • •